

## Environmentally safe corrosion inhibition of the Cu–Ni alloys in acidic sulfate solutions

WAHEED A. BADAWY<sup>1</sup>, KHALED M. ISMAIL<sup>1</sup> and AHLAM M. FATHI<sup>2,\*</sup>

<sup>1</sup>Department of chemistry, Faculty of Science, Cairo University, Giza, Egypt

<sup>2</sup>Department of Physical Chemistry, National Research Centre, Giza, Egypt

(\*author for correspondence, e-mail: wbadawy50@hotmail.com, wbadawy@main-scc.cairo.eun.eg)

Received 16 August 2004; accepted in revised form 10 March 2005

**Key words:** Copper–nickel alloys, corrosion, corrosion inhibition, impedance, polarization

### Abstract

The corrosion and passivation behaviors of alloys with different Cu–Ni ratios were investigated in acidic sulfate solutions. The corrosion rate was calculated and the corrosion inhibition process was investigated using different amino acids as corrosion inhibitors. For these investigations conventional electrochemical techniques and electrochemical impedance spectroscopy (EIS) were used. Fitting of the experimental impedance data to theoretical values enables understanding of the corrosion inhibition mechanism and the suggestion of a suitable electrical model to explain the behavior of the alloys under different conditions. The investigation of the electrochemical behavior of alloys before and after the corrosion inhibition processes has shown that some amino acids like lysine have promising corrosion inhibition efficiency at very low concentrations. A model for the electrode/electrolyte interface during the corrosion inhibition processes was suggested and the validity of the model for the explanation of the corrosion inhibition phenomena was discussed.

### 1. Introduction

Copper–nickel alloys are extensively used in different industrial applications, such as ships, power stations, heat exchangers and generally in salt-water services. With relatively high Ni content (Cu–30Ni), the alloy is used under most polluted water conditions and in pipe lines in naval applications. The widespread use of these alloys depends on a combination of good corrosion resistance and excellent workability as well as high thermal and electrical conductivity [1, 2]. The electrochemical behavior of cupronickels with different nickel contents has been extensively studied [3–13]. An increase in nickel content in solutions with relatively high chloride ion concentration ( $[Cl^-] > 0.5$  M) improves the corrosion resistance of the alloy [14]. Nickel contents higher than 50% were found to decrease the corrosion currents compared to pure copper [15].

The increase in Ni content is relatively expensive and the alloy may suffer from selective leaching of Ni, especially in acid solutions [13]. Corrosion inhibition seems to be the only solution to overcome these problems. It is well known that the use of conventional corrosion inhibitors leads to environmental problems.

In this work some naturally occurring amino acids were used as inhibitors for the corrosion of two representative, widely used Cu–Ni alloys, namely, Cu–5Ni and Cu–65Ni

in acidic sulfate solutions. The corrosion rate was calculated and the corrosion inhibition process was investigated using the different amino acids as environmentally safe corrosion inhibitors. In acidic solutions amino acids are present in the protonated form. The adsorption of the protonated amino acid molecule is enhanced in the presence of halide ions [16]. Since chloride ions and to a lesser extent bromide ions are pitting initiators [17], the corrosion inhibition process was also investigated in presence of different concentration of iodide ions. For these investigations conventional electrochemical techniques and electrochemical impedance spectroscopy (EIS) were used. Fitting of the experimental impedance data to theoretical values enables understanding of the corrosion behavior and the suggestion of a suitable electrical model to explain the mechanisms of both the corrosion and inhibition processes at the alloy/solution interface.

### 2. Experimental details

The working electrodes were made from Cu–Ni rods and sheets, mounted into glass tubes by two-component epoxy resin leaving a surface area of  $0.2$  cm<sup>2</sup> to contact the solution. The materials used were commercial-grade Cu–Ni alloys of two different Ni contents (5 and 65

mass% Ni). The cell was a three-electrode all-glass cell, with a platinum counter electrode and saturated calomel reference electrode. Before each experiment, the working electrode was polished mechanically using successive grades of emery paper up to 1000 grit, rubbed with a smooth polishing cloth, then washed with triple distilled water and transferred quickly to the electrolytic cell. Electrochemical measurements were carried out in acidic sulfate solution (0.25 M Na<sub>2</sub>SO<sub>4</sub> + 0.05 M H<sub>2</sub>SO<sub>4</sub>, pH 2.0).

The electrochemical impedance investigations and polarization measurements were performed using the Zahner Elektrik IM6 electrochemical work station. The potentials were measured against and referred to the saturated calomel electrode (SCE). All cyclic voltammetry measurements were carried out using a scan rate of 10 mV s<sup>-1</sup>. For the calculation of the corrosion current density,  $i_{\text{corr}}$ , and the corrosion potential,  $E_{\text{corr}}$ , the potentiodynamic measurements were conducted at a scan rate of 1 mV s<sup>-1</sup>. The amino acids used in these investigations include:

1. Aliphatic amino acids; glycine, alanine and leucine.
2. Sulfur containing amino acids; cysteine.
3. Acidic amino acids; glutamic acid.
4. Basic amino acids; lysine and histidine.

The corrosion inhibition efficiency,  $\eta$ , was calculated from the values of the corrosion current densities of the alloy before and after the addition of the amino acid to the corrosive medium. Analytically pure potassium iodide was used to investigate the effect of iodide ions on the inhibition process. To achieve the best reproducibility, each experiment was carried out at least twice.

Details of the experimental procedures are described elsewhere [12, 18, 19].

### 3. Results and discussion

#### 3.1. Open-circuit potential measurements

The open-circuit potentials of the two alloys (Cu–5Ni and Cu–65Ni) in the absence and presence of amino acids were traced over 3 h from electrode immersion in the acidic sulfate solutions. In general, the steady state potential of the two alloys is reached within 120 min. Irrespective of the Ni content, the steady state potential is in the range of the open-circuit potential of pure copper (~–25 mV) [13]. Addition of the amino acids to the acidic sulfate produced little change in the open-circuit potential of the alloys. The addition of KI to the acidic sulfate solution containing the amino acid shifted the open-circuit potential in the negative direction. This negative shift was found to be dependent on the concentration of the iodide ion irrespective of the amino acid itself as can be seen from the values presented in Tables 1–4. This negative potential shift indicates that the iodide ions influence the active centers on the alloy surface and hence the corrosion rate, as will be discussed later.

#### 3.2. Effect of amino acid concentration on the corrosion rate of the alloys

The corrosion parameters of the two alloys in amino acid free 0.25 M Na<sub>2</sub>SO<sub>4</sub> at pH 2 and in the same

Table 1. Corrosion parameters for Cu–5Ni alloy in 0.25 M acidic Na<sub>2</sub>SO<sub>4</sub> in the presence of different concentrations of amino acids

[Inh]	Glycine			Alanine			Leucine			Lysine			Histidine			Glutamic acid			Cysteine		
	$E_{\text{corr}}$	$i_{\text{corr}}$	$\eta$	$E_{\text{corr}}$	$i_{\text{corr}}$	$\eta$	$E_{\text{corr}}$	$i_{\text{corr}}$	$\eta$	$E_{\text{corr}}$	$i_{\text{corr}}$	$\eta$	$E_{\text{corr}}$	$i_{\text{corr}}$	$\eta$	$E_{\text{corr}}$	$i_{\text{corr}}$	$\eta$	$E_{\text{corr}}$	$i_{\text{corr}}$	$\eta$
0.00	–32	2.55	–	–32	2.55	–	–32	2.55	–	–32	2.55	–	–32	2.55	–	–32	2.55	–	–32	2.55	–
0.01	–55	7.58	–197	–55	7.58	–87	–62	1.55	39	–88	2.51	1	–68	2.63	–3	–55	1.58	38	–75	1.99	22
0.05	–80	2.24	12	–55	3.01	–18	–65	3.98	–56	–90	2.39	6	–75	2.51	1	–55	3.50	–37	–80	2.24	12
0.10	–70	2.57	–0.7	–85	1.90	25	–65	4.26	–67	–90	2.24	12	–55	3.55	–39	–57	3.89	–67	–60	2.81	–10
0.20	–91	2.57	–0.7	–82	1.99	22	–65	4.26	–67	–90	1.57	38	–60	4.16	–63	–70	4.26	–68	–42	3.01	–18
2.00	–63	3.38	–32	–88	2.51	1	–68	5.01	–96	–82	2.24	12	–65	4.46	–75	–75	6.30	–147	–40	3.16	–24

[Inhibitor]/mM,  $E_{\text{corr}}$ /mV,  $i_{\text{corr}}$ /μA cm<sup>-2</sup>.

Table 2. Corrosion parameters for Cu–65Ni alloy in 0.25 M acidic Na<sub>2</sub>SO<sub>4</sub> in the presence of different concentrations of amino acids

[Inh]	Glycine			Alanine			Leucine			Lysine			Histidine			Glutamic acid			Cysteine		
	$E_{\text{corr}}$	$i_{\text{corr}}$	$\eta$	$E_{\text{corr}}$	$i_{\text{corr}}$	$\eta$	$E_{\text{corr}}$	$i_{\text{corr}}$	$\eta$	$E_{\text{corr}}$	$i_{\text{corr}}$	$\eta$	$E_{\text{corr}}$	$i_{\text{corr}}$	$\eta$	$E_{\text{corr}}$	$i_{\text{corr}}$	$\eta$	$E_{\text{corr}}$	$i_{\text{corr}}$	$\eta$
0.00	–25	5.6	–	–25	5.6	–	–25	5.6	–	–25	5.6	–	–25	5.6	–	–25	5.6	–	–25	5.6	–
0.01	–52	7.9	–40	–25	4.8	15	–40	8.3	–48	–40	5.3	6	–55	1.2	79	–35	8.9	–58	–33	3.9	31
0.05	–40	6.3	–12	–31	4.2	26	–40	5.6	00	–40	2.9	47	–40	4.8	15	–35	4.2	26	–45	3.3	41
0.10	–70	2.6	–0.7	–85	1.9	25	–65	4.4	–67	–90	2.2	12	–55	3.6	–39	–57	3.9	–67	–60	2.8	–10
0.20	–40	4.8	14	–37	6.0	–7	–45	4.8	14	–50	3.2	44	–27	7.4	–32	–44	7.1	–26	–62	2.6	54
2.00	–38	7.1	–26	–32	7.6	–35	–45	6.3	–12	–50	6.0	–7	–35	8.9	–58	–35	8.9	–58	–77	4.5	20

Table 3. Corrosion parameters for Cu-5Ni alloy in 0.25 M Na<sub>2</sub>SO<sub>4</sub> with a certain inhibitor concentration + different concentrations of KI

[KI]	0.05 mM Glycine			0.1 mM Alanine			0.01 mM Leucine			0.2 mM Lysine			0.05 mM Histidine			0.01 mM Glutamic			0.01 mM Cysteine		
	$E_{\text{corr}}$	$i_{\text{corr}}$	$\eta$	$E_{\text{corr}}$	$i_{\text{corr}}$	$\eta$	$E_{\text{corr}}$	$i_{\text{corr}}$	$\eta$	$E_{\text{corr}}$	$i_{\text{corr}}$	$\eta$	$E_{\text{corr}}$	$i_{\text{corr}}$	$\eta$	$E_{\text{corr}}$	$i_{\text{corr}}$	$\eta$	$E_{\text{corr}}$	$i_{\text{corr}}$	$\eta$
0.00	-80	2.24	12	-85	1.90	25	-62	1.55	39	-90	1.57	38	-40	4.80	15	-55	1.58	38	-75	1.99	22
0.05	-125	1.12	56	-132	1.02	60	-125	1.90	25	-116	1.82	29	-112	1.13	56	-104	1.41	45	-136	2.24	12
0.10	-140	1.26	50	-138	1.23	52	-140	0.90	65	-95	1.78	30	-59	1.12	56	-113	0.93	63	-143	1.16	54
0.50	-175	1.31	49	-180	1.31	49	-180	1.40	45	-171	1.44	43	-192	1.78	30	-135	1.55	39	-165	1.35	47
1.00	-205	1.99	22	-220	1.51	41	-200	1.50	41	-186	2.14	16	-200	1.78	30	-195	1.66	34	-186	1.44	43
5.00	-222	1.99	22	-250	1.58	38	-220	2.50	1	-216	2.24	12	-242	1.95	23	-200	1.99	21	-216	2.51	1

[KI]/mM,  $E_{\text{corr}}$ /mV,  $i_{\text{corr}}$ / $\mu\text{A cm}^{-2}$ .Table 4. Corrosion parameters for Cu-65Ni alloy in 0.25 M Na<sub>2</sub>SO<sub>4</sub> with a certain inhibitor concentration + different concentrations of KI

[KI]	0.2 mM Glycine			0.05 mM Alanine			0.2 mM Leucine			0.05 mM Lysine			0.01 mM Histidine			0.05 mM Glutamic			0.2 mM Cysteine		
	$E_{\text{corr}}$	$i_{\text{corr}}$	$\eta$	$E_{\text{corr}}$	$i_{\text{corr}}$	$\eta$	$E_{\text{corr}}$	$i_{\text{corr}}$	$\eta$	$E_{\text{corr}}$	$i_{\text{corr}}$	$\eta$	$E_{\text{corr}}$	$i_{\text{corr}}$	$\eta$	$E_{\text{corr}}$	$i_{\text{corr}}$	$\eta$	$E_{\text{corr}}$	$i_{\text{corr}}$	$\eta$
0.00	-40	4.80	14	-31	4.20	26	-45	4.80	14	-40	2.90	47	-55	1.20	79	-35	4.20	26	-62	2.60	54
0.05	-95	1.12	80	-95	0.89	84	-100	2.24	60	-116	2.82	49	-90	1.12	80	-63	0.95	83	-	-	-
0.10	-115	0.63	88	-100	1.12	80	-140	2.24	60	-140	2.04	64	-85	1.17	79	-95	0.79	86	-125	2.51	55
0.50	-150	1.58	72	-140	1.51	73	-125	1.00	82	-140	1.51	73	-108	0.56	90	-155	0.75	87	-125	2.51	55
1.00	-150	1.90	66	-150	1.78	68	-145	0.50	91	-161	1.46	74	-163	1.30	77	-150	1.46	74	-133	1.16	79
5.00	-170	3.16	44	-180	1.99	65	-160	1.99	65	-164	0.56	90	-200	1.57	72	-196	1.46	74	-129	0.71	87

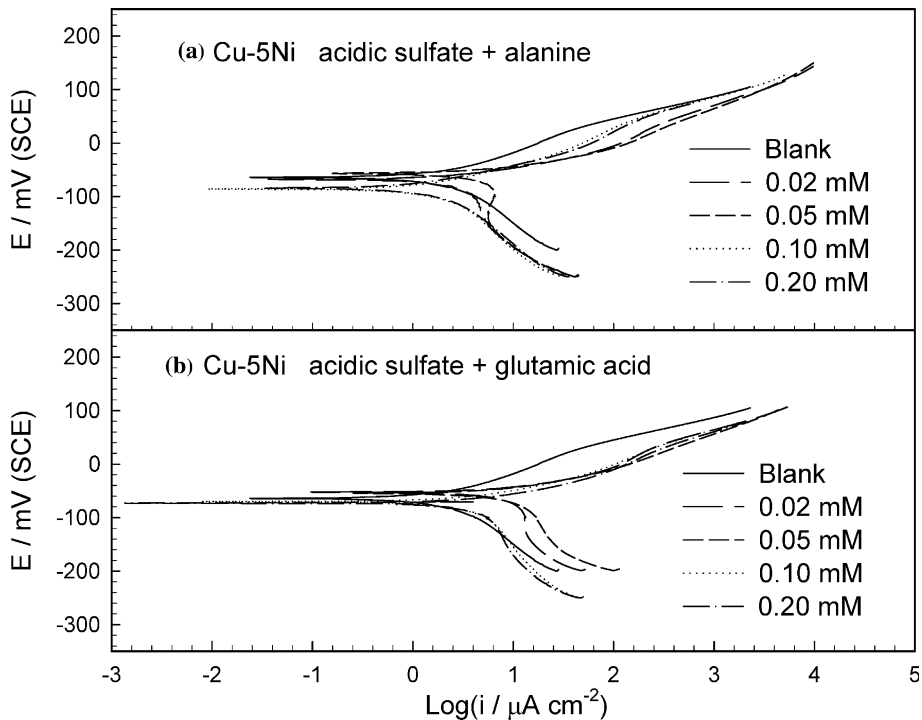


Fig. 1. Potentiodynamic polarization curves for Cu-5Ni alloy in 0.25 M acidic sulfate solution with different concentrations of (a) alanine and (b) glutamic acid.

solution containing different concentrations of the amino acids were obtained from potentiodynamic polarization experiments. Figures 1 and 2 present potentiodynamic polarization curves for Cu-5Ni and Cu-65Ni in acidic sulfate containing different concentrations of two representative amino acids, namely alanine (Figures 1a and 2a) and glutamic acid (Figures 1b and

2b). Four different concentrations of the amino acid, namely 0.02, 0.05, 0.10 and 0.20 mM as well as the amino acid free solution are presented in these figures. In general, the presence of different concentrations of the amino acid alone in the acidic solution did not show a remarkable effect on the potentiodynamic polarization curves. In some cases, the amino acid increases the

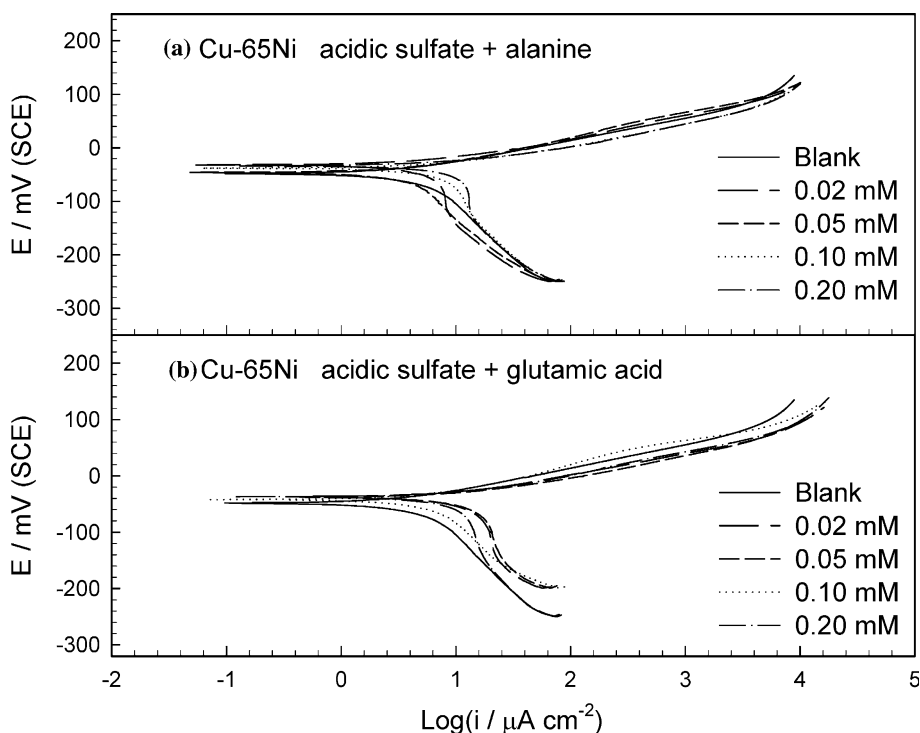


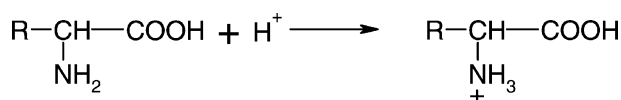
Fig. 2. Potentiodynamic polarization curves for Cu-65Ni alloy in 0.25 M acidic sulfate solution with different concentrations of (a) alanine and (b) glutamic acid.

anodic currents. This means that it accelerates the corrosion rate rather than inhibiting it. The values of the corrosion parameters, corrosion current density,  $i_{\text{corr}}$ , corrosion potential,  $E_{\text{corr}}$ , and the corrosion resistance,  $R_{\text{corr}}$ , were calculated for both Cu-5Ni and Cu-65Ni alloys with the different amino acids and are presented in Tables 1 and 2, respectively. The calculated values show that the corrosion potential did not shift remarkably from the initial value of the amino acid free acidic sulfate solution. In some cases, a negative shift of about 50 mV was recorded.

The corrosion inhibition efficiency,  $\eta$ , was calculated for the different amino acids at different concentrations according to:

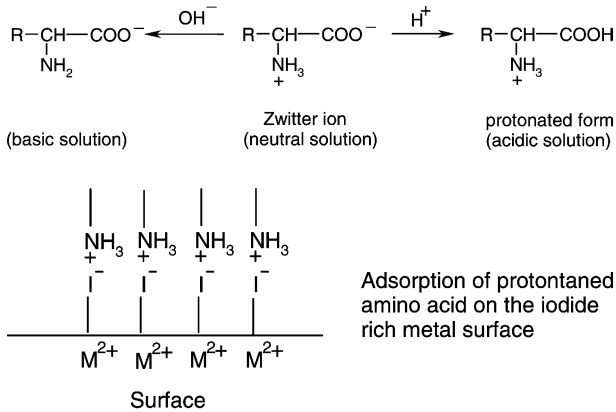
$$\eta = \frac{i_{\text{corr}} - i_{\text{corr(inh)}}}{i_{\text{corr}}} \times 100 \quad (1)$$

where  $i_{\text{corr}}$  is the corrosion current density for the alloy in inhibitor free acidic sulfate solution and  $i_{\text{corr(inh)}}$  is the value after the addition of a certain amount of inhibitor under the same conditions. The values of  $\eta$  in all cases are also included in Tables 1 and 2. The values of  $\eta$  presented in these tables show that many of the investigated amino acids accelerate the corrosion process rather than inhibiting it, therefore they cannot be used alone as inhibitors. The inhibition effect of the amino acid is due to the adsorption of its molecules on the alloy surface [20], and the adsorption process depends on both the nature and state of the surface, and also on the nature and properties of the amino acid. In general, the amino acid occurs in its protonated form in acidic solution i.e.



The protonated form can be attracted to the cathodic sites on the alloy surface. The presence of negative ions like iodide ions may enhance the adsorption of the amino acid [16]. For this reason the effect of iodide ions on the corrosion inhibition efficiency was also investigated. Representative potentiodynamic polarization curves of these measurements for Cu-5Ni and Cu-65Ni alloys are presented in Figures 3 and 4 for alanine and glutamic acid. The measurements were made for all amino acids using the optimum concentration of each and different concentrations of KI. The values of  $E_{\text{corr}}$ ,  $i_{\text{corr}}$ , and  $R_{\text{corr}}$ , and also the inhibition efficiency,  $\eta$ , in each case were calculated and are presented in Tables 3 and 4. In all cases, the corrosion potential shifts negatively more than 100 mV, indicating that the addition of the iodide influences the alloy surface and hence the corrosion rate. The corrosion current density decreases as the concentration of iodide ions increases.

The synergistic effect between the amino acids and iodide ions leads to a stabilized adsorption of the amino acid molecules on the alloy surface through the iodide ions. The iodide ions are adsorbed on the active sites of the surface where the corrosion process occurs leading to a negatively charged surface, which is suitable for the adsorption of the protonated form of the amino acid according to:



The negative shift of the corrosion potential in the presence of  $\text{I}^-$  ions can be attributed to the adsorption process. The adsorption of amino acid on the alloy surface free from the iodide is not stable [21]. In the iodide free solutions, the carboxylic group of the amino acid is adsorbed on the anodic sites through the electron lone pairs of the carbonyl group and hence no remarkable negative shift of the corrosion potential occurs [22].

Generally, the adsorption process depends on two essential factors, the molecular structure of the adsorbent and the surface properties of the alloy [22, 23]. As the chain length of the amino acid increases the inhibition efficiency increases. A longer chain length is capable of covering a larger area of the surface preventing its contact with the corrosive medium. This explains why lysine gives the highest corrosion inhibition efficiency, which reaches 96% with Cu-65Ni. The

presence of chain branching prevents the close packing of the inhibitor molecules and hence lower inhibition efficiency is recorded. This explains the lower  $\eta$  values recorded for small molecules like glycine or branched structures like leucine. In branched molecules the carbonyl group and the amino group of the amino acid molecule do not exist in the same plane due to rotation of the carboxylic group around the bond between the  $\alpha$  carbon atom and the carbon of the carboxylic group which results in the reduction of the adsorption capability [24], and so lysine is the most effective inhibitor. Comparison of the data presented in Tables 1 and 2 (or 3 and 4), it is clear that the inhibition efficiency for the corrosion of Cu-65Ni is remarkably larger than that of Cu-5Ni for the same amino acid and same concentration. In Cu-65Ni, the number of Ni-sites on the alloy surface is very large compared to Cu-5Ni, which reduces the possibility of oxidation of the amino acid molecules on the alloy surface and so the adsorption of these molecules becomes stronger on the Ni-rich surface, leading to higher corrosion inhibition efficiency [25].

### 3.3. Impedance measurements

To confirm the potentiodynamic polarization experiments, electrochemical impedance spectroscopic investigations of both alloys in inhibitor free and inhibitor containing acid sulfate solutions were carried out. Electrochemical impedance is a powerful tool in the investigation of the corrosion and adsorption phenomena [26]. It enables the fitting of the experimental

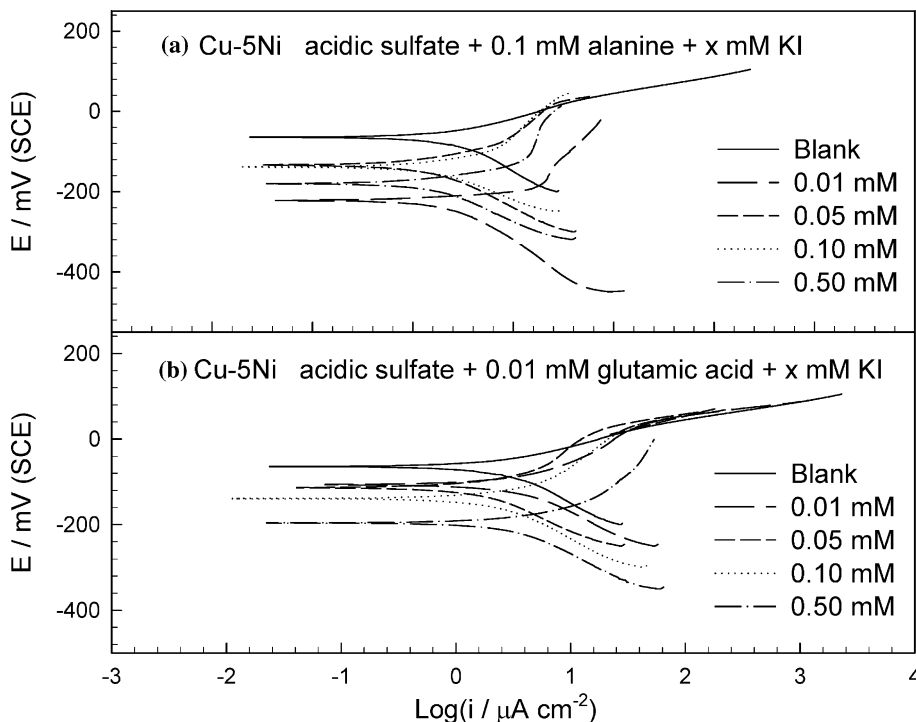


Fig. 3. Potentiodynamic polarization curves for Cu-5Ni alloy in 0.25 M acidic sulfate solution with (a) 0.1 mM alanine and (b) 0.01 mM glutamic acid + different concentrations of KI.

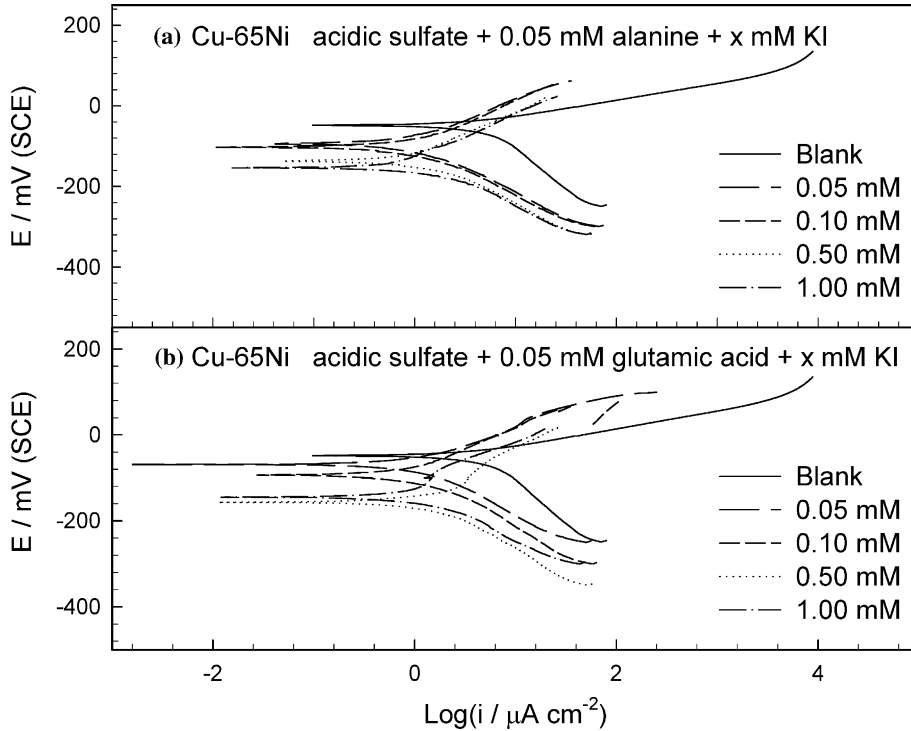


Fig. 4. Potentiodynamic polarization curves for Cu-65Ni alloy in 0.25 M acidic sulfate solution with (a) 0.05 mM alanine and (b) 0.05 mM glutamic acid + different concentrations of KI.

results to a pure electronic model to represent the electrochemical system under investigation. The correlation of the experimental impedance plot to an equivalent circuit enables the verification of the mechanistic model for the system. Such a correlation leads to the calculation of the numerical values corresponding to physical and/or chemical properties of the electrochemical system [26, 27]. The impedance data of Cu-5Ni and Cu-65Ni after 3 h immersion in the different electrolytes are presented as Bode plots in Figure 5a and b. Data fitting was carried out using a complex non-linear least squares procedure.

The Bode plots for Cu-5Ni alloy after 3 h immersion in inhibitor free acidic sulfate, acidic sulfate containing 0.01 mM leucine and acidic sulfate containing 0.01 mM leucine + 0.1 mM KI are presented in Figure 5a. The electrode impedance increases remarkably in the presence of the iodide ion, indicating that the electrode surface becomes passive. The corrosion resistance increases from  $47 \Omega \text{ cm}^2$  in inhibitor free acidic sulfate solution to  $6680 \Omega \text{ cm}^2$  in the presence of leucine and iodide. Also, the phase maximum at intermediate frequencies broadens in the presence of iodide, which indicates the presence of a protective layer [28]. The impedance data were analyzed using an equivalent circuit model presented in Figure 6. In this model equivalent circuit parameters were introduced to account for the electrode capacitance,  $C$ , the polarization resistance,  $R_p$ , the ohmic drop in the electrolyte,  $R_\Omega$ , adsorption film resistance,  $R_{ad}$ , adsorption film capacitance,  $C_{ad}$ , and a Warburg impedance parameters,  $Z_w$ , to account for the diffusion process.

For simple equivalent circuit models, where the capacitance, polarization resistance, and solution resistance, are only considered, the electrode impedance,  $Z$ , is represented by the dispersion formula:

$$Z = R_\Omega + \frac{R_p}{1 + (2\pi f R_p C)^\alpha} \quad (2)$$

where  $\alpha$  denotes an empirical parameter ( $0 \leq \alpha \leq 1$ ) and  $f$  is the frequency in Hz. This takes into account deviation from ideal capacitor behavior in terms of time constants due to surface inhomogeneities, roughness effects and adsorption phenomena [29, 30]. The calculated equivalent circuit parameters for Cu-5Ni and Cu-65Ni after 3 h immersion in the different electrolytes are presented in Tables 5 and 6. The values presented in Table 5 show that  $R_{ad}$  increases from  $0.32 \text{ k}\Omega \text{ cm}^2$  in inhibitor free solution to  $15.1 \text{ k}\Omega \text{ cm}^2$  when the solution contains 0.01 mM leucine + 0.1 mM KI. The addition of leucine alone did not show such dramatic effect,  $R_{ad}$  increases from  $0.32$  to  $0.81 \text{ k}\Omega \text{ cm}^2$  only. The value of  $1/C_{ad}$  increases, which accounts for the adsorption layer thickness [17, 31]. This means that a thicker adsorption layer is formed. The effect of the immersion time on the corrosion resistance of the alloy in the presence and absence of iodide ions is presented as Bode plots in Figure 7a and b. The equivalent circuit parameters in each case were also calculated and are presented in Tables 7 and 8. The values of both  $R_{ad}$  and  $1/C_{ad}$ , increase with increase in immersion time up to 60 min, which means that the immersion of the alloy for  $\sim 1$  h in the solution containing the inhibitor leads to the formation

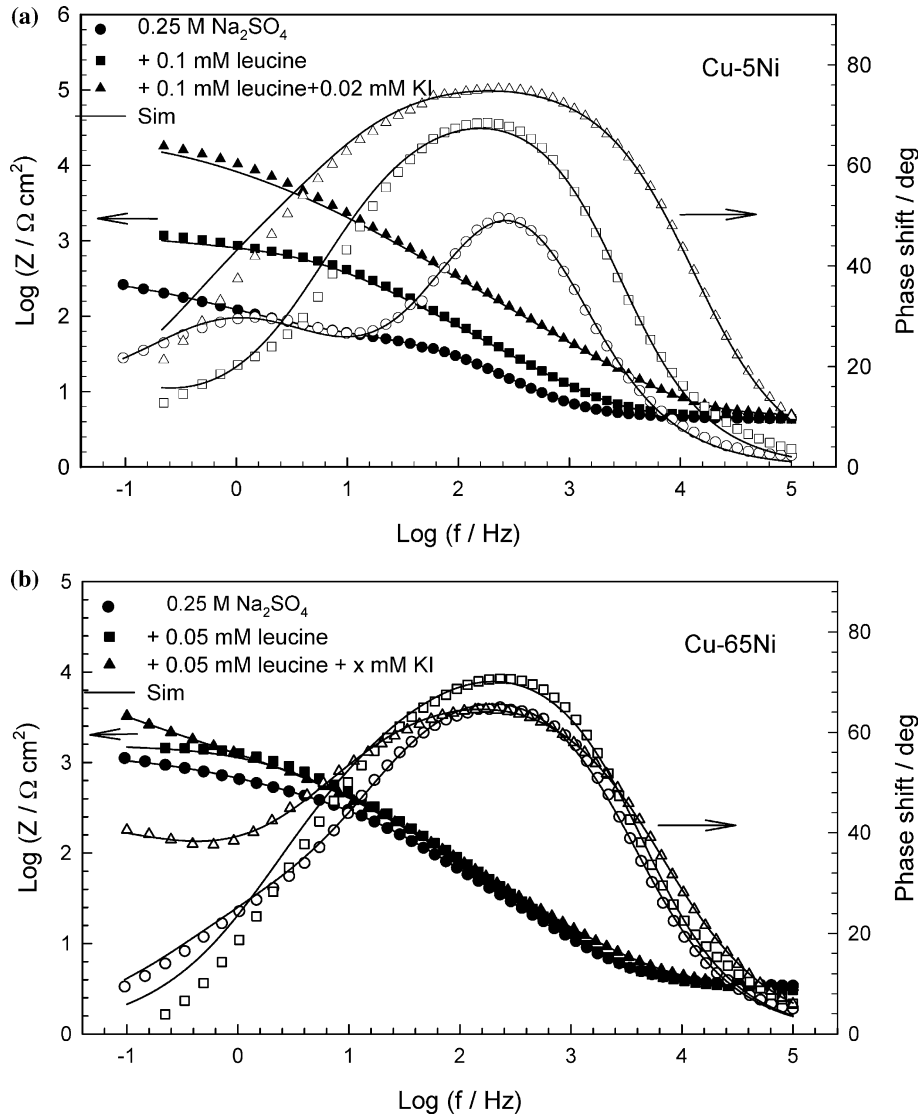


Fig. 5. (a) Bode plots for Cu-5Ni alloy after 180 min of immersion in 0.25 M acidic sulfate with inhibitor (and KI) at 25 °C. (b) Bode plots for Cu-65Ni alloy after 180 min of immersion in 0.25 M acidic sulfate with inhibitor (and KI) at 25 °C.

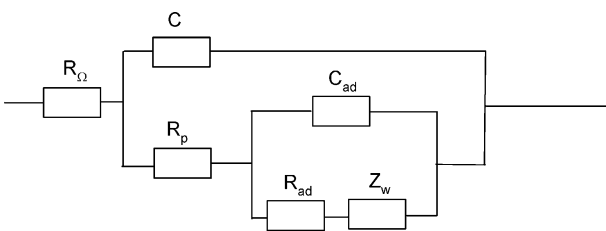


Fig. 6. Equivalent circuit used in the fitting of the impedance data of Cu-Ni alloys at different conditions,  $R_{\Omega}$  = solution resistance,  $R_p$  = polarization resistance,  $C$  = electrode capacitance,  $R_{ad}$  = adsorbed layer resistance,  $C_{ad}$  = adsorbed layer capacitance, and  $Z_w$  = Warburg impedance.

of a thicker adsorption layer which protects and increases the corrosion inhibition efficiency. This result is better seen on Figure 8a and b for Cu-5Ni alloy in acidic sulfate solution containing 0.01 mM leucine (Figure 8a) and that containing 0.01 mM leucine + 0.1 mM KI (Figure 8b).

The same experiments were carried out with Cu-65Ni, the corresponding impedance data were recorded and the equivalent circuit parameters were also calculated. The results for Cu-65Ni show the same trend as those recorded for Cu-5Ni and presented in Figure 7a and b. In all cases, the calculated values for  $\alpha$  deviate

Table 5. Equivalent circuit parameters for Cu-5Ni in 0.25 M  $\text{Na}_2\text{SO}_4$ , pH 2 without and with inhibitor (and KI)

[Leucine]/mM	$R_{\Omega}/\Omega$	$C/\mu\text{F cm}^{-2}$	$\alpha_1$	$R_p/\Omega \text{ cm}^2$	$C_{ad}/\mu\text{F cm}^{-2}$	$\alpha_2$	$R_{ad}/\text{k}\Omega \text{ cm}^2$	$Z_w/\text{k}\Omega \text{ s}^{-1/2}$
0.00	22.0	34.0	0.87	47	70	0.62	0.32	0.08
0.01	22.5	14.6	0.91	61.8	2.5	0.60	0.81	1.6
0.01 + 0.1 mM KI	23.6	3.6	0.86	6680	1.3	0.63	15.1	10.1

Table 6. Equivalent circuit parameters for Cu-65Ni in 0.25 M Na<sub>2</sub>SO<sub>4</sub>, pH 2 without and with inhibitor (and KI)

[Leucine]/mM	$R_{\Omega}/\Omega$	$C/\mu\text{F cm}^{-2}$	$\alpha_1$	$R_p/\Omega \text{ cm}^2$	$C_{ad}/\mu\text{F cm}^{-2}$	$\alpha_2$	$R_{ad}/\text{k}\Omega \text{ cm}^2$	$Z_w/\text{k}\Omega \text{ s}^{-1/2}$
0.00	15.9	15.75	0.82	575	27.34	0.61	0.803	0.01
0.01	16.4	9.10	0.85	882	8.20	0.60	3.40	0.12
0.01 + 0.02 mM KI	17.0	15.80	0.78	586	0.30	0.61	2.18	4.96

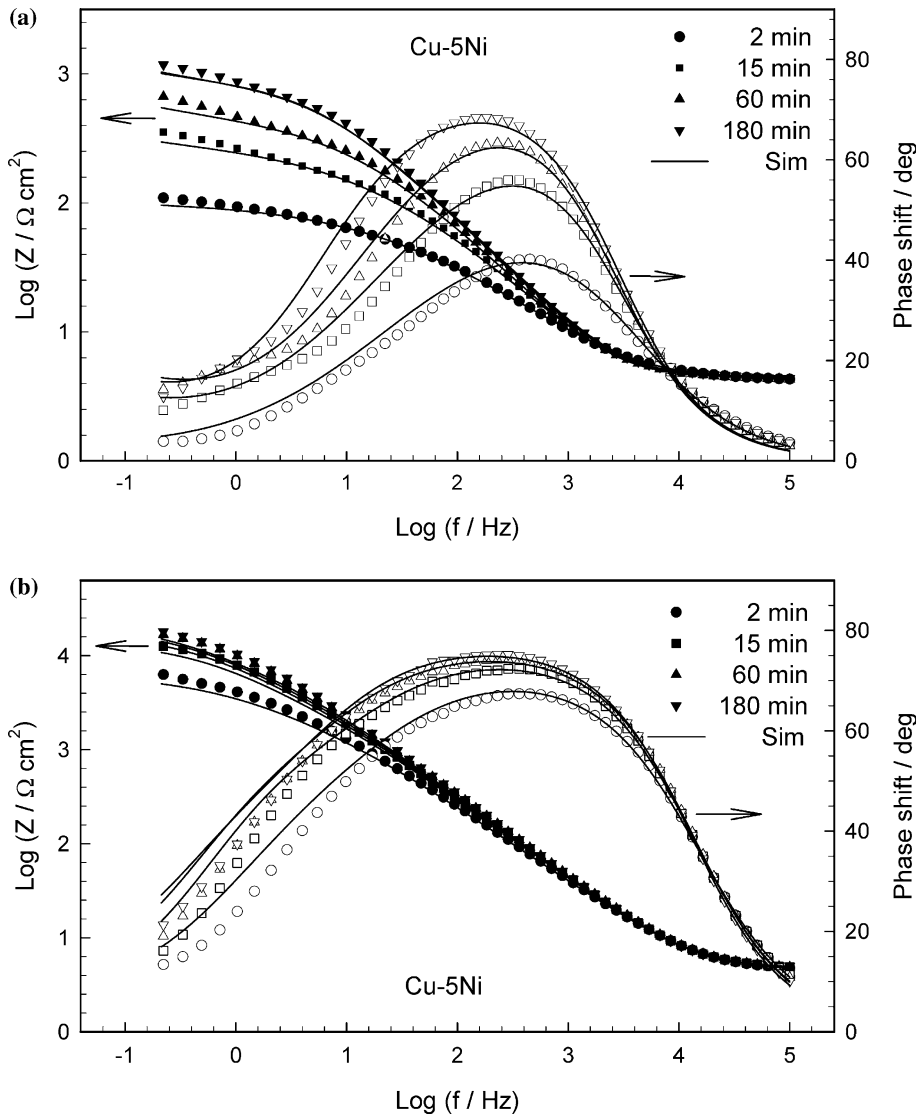


Fig. 7. (a) Bode plots for Cu-5Ni alloy after different time of immersion in acidic sulfate solution + 0.1 mM leucine at 25 °C. (b) Bode plots for Cu-5Ni alloy after different time of immersion in acidic sulfate solution + 0.1 mM leucine + 0.02 mM KI at 25 °C.

Table 7. Equivalent circuit parameters for Cu-5Ni after different time of immersion in 0.25 M Na<sub>2</sub>SO<sub>4</sub> (pH 2) + 0.01 mM leucine at 25 °C

Time/min	$R_{\Omega}/\Omega$	$C/\mu\text{F cm}^{-2}$	$\alpha_1$	$R_p/\Omega \text{ cm}^2$	$C_{ad}/\mu\text{F cm}^{-2}$	$\alpha_2$	$R_{ad}/\text{k}\Omega \text{ cm}^2$	$Z_w/\text{k}\Omega \text{ s}^{-1/2}$
2	21.5	11.1	0.89	1.49	11.70	0.50	0.09	17
15	21.9	13.7	0.93	4.10	5.50	0.50	0.28	345
30	21.9	14.3	0.92	6.99	3.90	0.50	0.38	717
60	22.1	14.9	0.92	10.40	2.98	0.50	0.48	980
120	22.4	13.8	0.91	59.00	2.60	0.60	0.80	1945
180	22.5	14.6	0.91	61.80	2.50	0.60	0.81	1600



Table 8. Equivalent circuit parameters for Cu–5Ni after different time of immersion in 0.25 M Na<sub>2</sub>SO<sub>4</sub> (pH 2) + 0.01 mM leucine + 0.1 mM KI at 25 °C

Time/min	$R_{\Omega} / \Omega$	$C / \mu\text{F cm}^{-2}$	$\alpha_1$	$R_p / \Omega \text{ cm}^2$	$C_{\text{ad}} / \mu\text{F cm}^{-2}$	$\alpha_2$	$R_{\text{ad}} / \text{k}\Omega \text{ cm}^2$	$Z_W / \text{k}\Omega \text{ s}^{-1/2}$
2	22.0	4.0	0.81	1.89	1.55	0.57	4.2	2.1
15	22.7	3.7	0.84	3.95	1.40	0.66	9.5	4.5
30	22.9	3.7	0.85	4.90	1.35	0.66	11.6	5.9
60	22.9	3.6	0.85	6.00	1.30	0.64	13.1	7.7
120	22.5	3.6	0.85	6.30	1.30	0.64	14.2	8.5
180	23.6	3.6	0.86	6.70	1.30	0.63	15.1	10.1

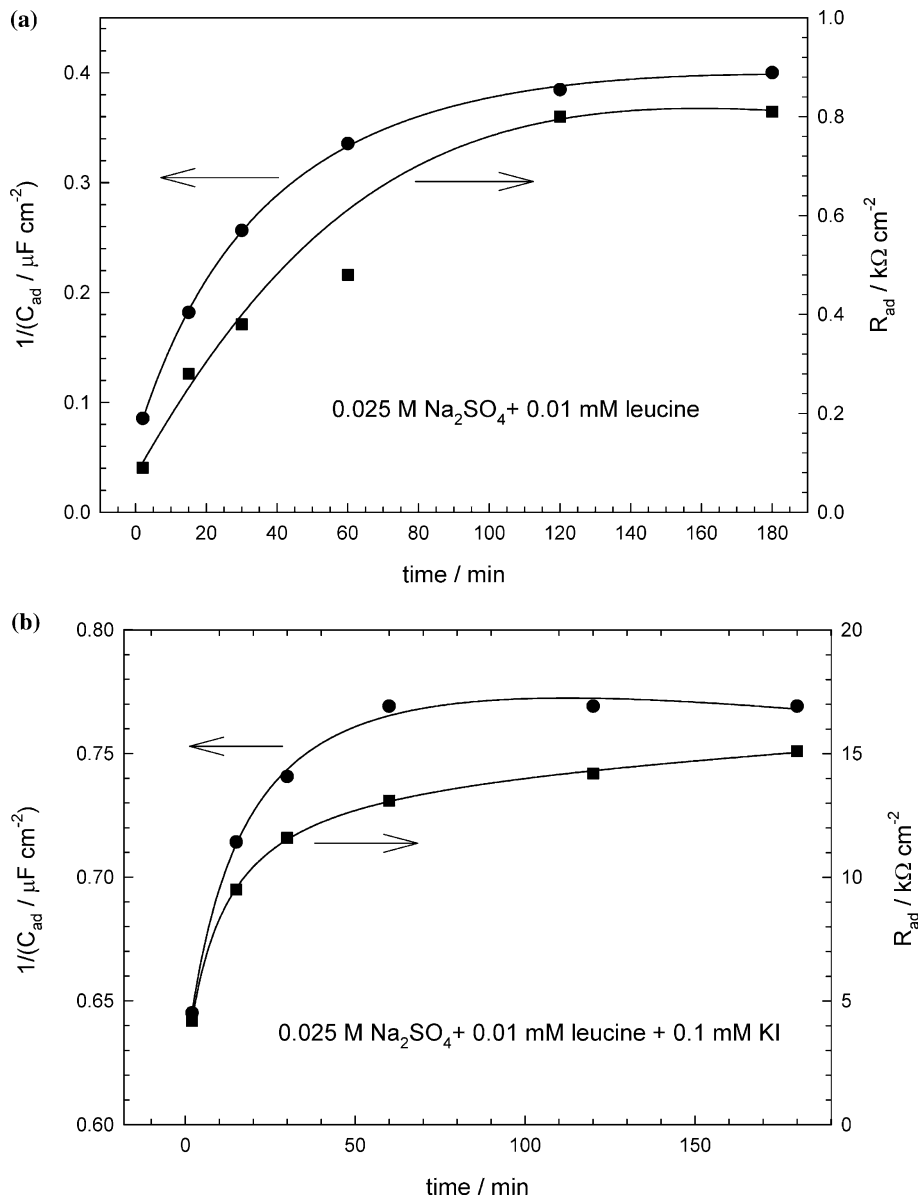


Fig. 8. Variation of  $R_{\text{ad}}$  and  $1/C_{\text{ad}}$  with time for Cu–5Ni alloy in acidic sulfate solution. (a) Containing 0.01 mM leucine (b) containing 0.01 mM leucine + 0.1 mM KI.

from 1 ( $\alpha_1 \approx 0.82$  to  $0.92$  and  $\alpha_2 \approx 0.5$  to  $0.66$ ) which indicates a heterogeneous surface [18, 29, 32]. The values of  $R_{\text{ad}}$  and  $1/C_{\text{ad}}$  for Cu–65Ni are remarkably higher than those for Cu–5Ni in the same solution. The

relatively higher adsorption resistance and thicker adsorption film formed on Cu–65Ni can be attributed to the large number of Ni-sites occurring on the Cu–65Ni surface compared to that on Cu–5Ni where the

possibility of oxidation of amino acid on the Cu-sites decreases [25].

#### 4. Conclusions

The corrosion and corrosion inhibition of the Cu–Ni alloys depend on the Ni content and the structure of the amino acid used. Long chain non-branched molecules are more effective in corrosion inhibition. The surface adsorption of amino acids in acidic solutions is enhanced in the presence of small amounts (0.1 mM) of iodide ions. Alloys of higher nickel content have thicker and more resistive adsorption layers.

#### References

1. P.T. Gilbert, in L.L. Shreir, R.A. Jarman and G.T. Burstein (Eds.) 'Corrosion: Metal/Environment Reaction', 3rd edn. (Butterworth-Heinemann Ltd, Linacre House, Jordan Hill, Oxford, reprinted 1995), p. 4:38 and 4:58.
2. D.A. Jones 'Principles and Prevention of Corrosion', 2nd edn. (Prentice Hall, Upper Saddle River, NJ, 1996), pp. 518–520.
3. R.E. Hummel and R.J. Smith, *Corros. Sci.* **28** (1988) 279.
4. J.A. Ali and J.R. Ambrose, *Corros. Sci.* **32** (1991) 799.
5. H.P. Hack and H.W. Pickering, *J. Electrochim. Soc.* **138** (1991) 690.
6. R. Zaroni, G. Gusmano, G. Montesperelli and E. Traversa, *Corrosion* **48** (1992) 404.
7. P. Druska and H.-H. Strehblow, *Corros. Sci.* **38** (1996) 1369.
8. J.M. Maciel and S.M.L. Agostinho, *J. Appl. Electrochim.* **30** (2000) 981.
9. R.S. Goncalves, D.S. Azambuja and A.M.S. Lucho, *Corros. Sci.* **44** (2002) 467.
10. W.A. Badawy; 21st Annual Egyptian Corrosion Society Conference, 'Sharm El-Sheikh Egypt, 17–20 December, 2002.
11. K.M. Ismail, A.M. Fathi and W.A. Badawy, *Corrosion* **60** (2004) 795.
12. K.M. Ismail, A.M. Fathi and W.A. Badawy, *J. Appl. Electrochem.* **34** (2004) 223–231.
13. K.M. Ismail, A.M. Fathi and W.A. Badawy; *Corros. Sci.* **47** (2005).
14. I. Milosev and M. Metikos-Hukovic, *Electrochim. Acta* **42** (1997) 1537.
15. A.N. Kamkin, A.D. Davydov, Zhou Guo-Ding and V.A. Marichev, *Russ. J. Electrochem.* **35** (1999) 531.
16. K.D. Allabergenov and F.K. Kurbanov, *Zashch. Met.* **15** (1979) 472.
17. A.I. Munoz, J.G. Anton, J.L. Guinon and V.P. Herranz, *Electrochim. Acta* **50** (2004) 957.
18. K.M. Ismail and W.A. Badawy, *J. Appl. Electrochem.* **30** (2000) 1303.
19. K.M. Ismail, A.A. El-Moneim and W.A. Badawy, *J. Electrochem. Soc.* **148** (2001) C81.
20. G. Bereket and A. Yurt, *Corros. Sci.* **43** (2001) 1179.
21. Y. Fengn, K.S. Siow, W.K. Teo and A.K. Hsieh, *Corros. Sci.* **41** (1999) 829.
22. N. Hajjaji, I. Rico, A. Srhiri, A. Lattes, M. Soufiaoui and A. Ben-Bachir, *Corros. Sci.* **49** (1993) 326.
23. A. Popova, E. Sokolova and S. Raicherva, *Khimia I industria* **2** (1988) 72.
24. A. Popova, E. Sokolova and S. Raicherva, *Khimia I industria* **6** (1987) 275.
25. I. Yeo and D.C. Johnson, *J. Electroanal. Chem.* **495** (2001) 110.
26. J.R. Macdonald, 'Impedance Spectroscopy', 3rd edn. (John Wiley & Sons, New York, 1987).
27. W.A. Badawy, F.M. Al-Kharafi and A.S. El-Azab, *Corros. Sci.* **41** (1999) 709.
28. W.A. Badawy, S.S. El-Egamy and Kh.M. Ismail, *Brit. Corr. J.* **28** (1993) 133.
29. K. Hladky, L.M. Calow and J.L. Dawson, *Brit. Corr. J.* **15** (1980) 20.
30. J. Hitzig, J. Titz, K. Juettner, W.J. Lorenz and E. Schmidt, *Electrochim. Acta* **29** (1984) 287.
31. J.W. Diggle, T.C. Downie and C.W. Goulding, *Electrochim. Acta* **15** (1970) 1079.
32. A.E. Bohe, J.R. Vilche, K. Juettner, W.J. Lorenz and W. Paatsch, *Electrochim. Acta* **34** (1989) 1443.